J Bioenerg Biomembr (2013) 45:551–559
DOI 10.1007/s10863-013-9523-y

Formation of superoxide anion and carbon-centered radicals by photosystem II under high light and heat stress—EPR spin-trapping study

Arjun Tiwari · Marek Rác · Pavel Pospíšil

Received: 21 March 2013 / Accepted: 19 July 2013 / Published online: 11 August 2013

Abstract In this study, electron paramagnetic resonance spin-trapping spectroscopy was used to study the light-induced production of superoxide anion ($O_2^{\bullet-}$) and carbon-centered ($R^{\bullet}$) radicals by Photosystem II (PSII). It is evidenced here that exposure of PSII membranes to high light (2,000 μmol photons m^{-2} s^{-1}) or heat (47 °C) treatments prior to the illumination suppressed $O_2^{\bullet-}$ production, while $R^{\bullet}$ was formed. Formation of $R^{\bullet}$ in the both high light- and heat-treated PSII membranes was enhanced by DCMU. Removal of molecular oxygen by glucose/glucose oxidase/catalase system and $O_2^{\bullet-}$ scavenging by exogenous superoxide dismutase completely suppressed carbon-centered radical formation. It is proposed here that the oxidation of polyunsaturated fatty acids and amino acids by $O_2^{\bullet-}$ on the electron acceptor side of PSII results in the formation of $R^{\bullet}$, known to initiate a cascade reaction leading to the lipid peroxidation and protein degradation, respectively.

Keywords Heat stress · Photoinhibition · Photosystem II · Reactive oxygen species · Redox potential

Abbreviations

*E*m	Midpoint redox potential
MES	2-[N-Morpholino]ethanesulfonic acid
PSII	Photosystem II
SOD	Superoxide dismutase
Q_A	Primary plastoquinone electron acceptor of PSII
Pheo	Pheophytin - primary electron acceptor of PSII
DCMU	3-(3,4-dichlorophenyl)-1,1-dimethylurea
EMPO	5-ethoxycarbonyl-5-methyl-1-pyrroline *N*-oxide

A. Tiwari · M. Rác · P. Pospíšil (✉)
Department of Biophysics, Centre of the Region Haná for Biotechnological and Agricultural Research, Faculty of Science, Palacký University, Šlechtitelů 11, 783 71 Olomouc, Czech Republic
e-mail: pospip@prfnw.upol.cz

Introduction

Exposure of plant to environmental stresses such as high light and high temperature leads to the oxidative stress connected to the formation of potentially damaging reactive oxygen species (ROS) (Hideg 1999; Hideg et al. 1994, 1995; Krieger et al. 1998; Foyer 2001; Apel and Hirt 2004). Superoxide anion radical ($O_2^{\bullet-}$) is the main ROS known to initiate the cascade reactions leading to the formation of hydrogen peroxide (H_2O_2) and hydroxyl radical ($HO^{\bullet}$). In chloroplasts, $O_2^{\bullet-}$ is produced mainly by photosystem I (PSI) and photosystem II (PSII), the former being considered as the main source of ROS in the thylakoid membrane (Asada 2006). However, under certain conditions such as limitation of electron transfer reactions, PSII might contribute to the overall production of $O_2^{\bullet-}$ in the thylakoid membrane.

Several lines of evidence have been provided that $O_2^{\bullet-}$ is formed by reduction of molecular oxygen on the electron acceptor side of PSII (Pospíšil 2009, 2012). The primary electron acceptor $Pheo^{\bullet-}$ (Ananyev et al. 1994) and primary quinone electron acceptor $Q_A^{\bullet-}$ (Cleland and Grace 1999) were proposed to serve as the reductants of molecular oxygen. From thermodynamic point of view, $Pheo^{\bullet-}$ has the highest reduction power (*E*m=− 610 mV, pH 7) and thus the reduction of molecular oxygen by $Pheo^{\bullet-}$ is highly favorable. However, from the kinetic reasons the reduction of molecular oxygen by $Pheo^{\bullet-}$ is less likely to occur due to the fast electron transfer from $Pheo^{\bullet-}$ to $Q_A^{\bullet-}$ (300–500 ps). The reduction of molecular oxygen by less reducing $Q_A^{\bullet-}$ (*E*m=− 80 mV, pH 7) is from kinetic reasons more likely due to slow reactions involving forward electron transfer from Q_A to Q_B (Pospíšil 2009). It has been proposed that the dominant reductant of molecular oxygen changes over the time course of photoinhibition in vitro (Pospíšil et al. 2004). The authors suggested that in the early phase, $Q_A^{\bullet-}$ serves as a reductant of molecular oxygen, whereas later $Pheo^{\bullet-}$ donates electron to molecular oxygen.

Reactive oxygen species are known to oxidize polyunsaturated fatty acid or amino acid forming carbon-centered radical ($R^{\bullet}$). The formation of $R^{\bullet}$ is known to initiate a cascade reaction leading to the lipid peroxidation and protein degradation (Eltsner 1987; Dean et al. 1997; Bhattacharjee 2005). The superoxide anion radical is weakly reactive; however, its protonated form $HO_2^{\bullet}$, known as perhydroxyl radical is considered to be more reactive. Although $O_2^{\bullet-}$ is relatively less reactive compared to another ROS, it could be potentially dangerous due to its tendency to get converted into more reactive species as $HO^{\bullet}$. It is well know that $HO^{\bullet}$ is produced by the reduction of H_2O_2 formed by spontaneous or superoxide dismutase-catalyzed dismutation of $O_2^{\bullet-}$ (Fridovich 1998; Halliwell and Gutteridge 2007). It has been demonstrated that $HO^{\bullet}$ is produced on the electron acceptor side of PSII by reduction of either ferric-hydroperoxo species formed by the interaction of $O_2^{\bullet-}$ with non-heme iron or by reduction of H_2O_2 formed by dismutation of $O_2^{\bullet-}$ (Pospíšil et al. 2004).

In this work, EPR spin-trapping technique was used to study light-induced production of $O_2^{\bullet-}$ and $R^{\bullet}$ by PSII previously exposed to high light or heat treatments. Evidence is provided that $HO_2^{\bullet}$ formed on the electron acceptor side of PSII oxidizes polyunsaturated fatty acids and amino acids leading to lipid peroxidation and protein degradation, respectively.

Materials and methods

Sample preparation

Spinach PSII membranes (BBY particles) were prepared using the method (Berthold et al. 1980) with the modifications described (Ford and Evans 1983). PSII membranes were stored at −80 °C in 0.4 M sucrose, 15 mM NaCl, 5 mM $MgCl_2$, 5 mM $CaCl_2$ and 40 mM Mes (pH 6.5) until use. In some measurement, 50 U ml^{-1} glucose oxidase, 5 mM glucose, 500 U ml^{-1} catalase, 10 μM DCMU, 500 U ml^{-1} SOD were added to PSII membranes before illumination. Stock solution of DCMU was prepared in ethanol. DCMU was added in PSII membranes to give a final concentration of 1 % (v/v) ethanol.

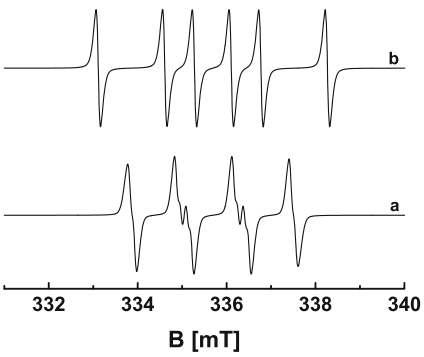

Fig. 1 Simulated EMPO-OOH (**a**) and EMPO-R (**b**) adduct EPR spectra obtained using the following hyperfine coupling constants: EMPO-OOH adduct (a^N=13.28 G; a^H=11.89 G and a^N=13.28 G; a^H=9.67 G) and EMPO-R adduct (a^N=15.42 G; a^H=22.30 G)

High light treatment

High light treatment was carried out by exposure of PSII membranes (150 μg Chl ml^{-1}) to continuous white light

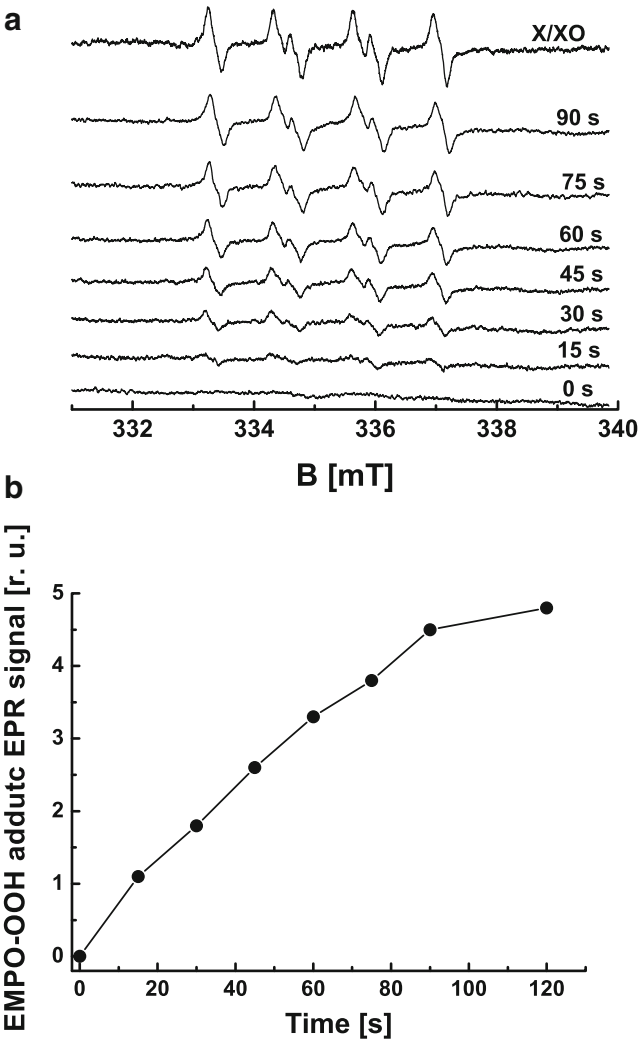

Fig. 2 **a** Light-induced EMPO-OOH adduct EPR spectra measured in PSII membranes after illumination for period indicated in figure. The spectra were recorded in the presence of 25 mM EMPO, 150 μg Chl ml^{-1}, 40 μM desferal and 25 mM MES (pH 6.5). The sample was illuminated with continuous white light of 1,000 μmol photons m^{-2} s^{-1}. The spectrum shown on the top was generated by incubation of mixtures contained 1 mM xanthine and 0.05 U ml^{-1} xanthine oxidase in the presence of 40 μM desferal and 25 mM EMPO. **b** Time profile of light-induced EMPO-OOH adduct EPR signal measured by various time period of illumination as shown in Fig. 2a

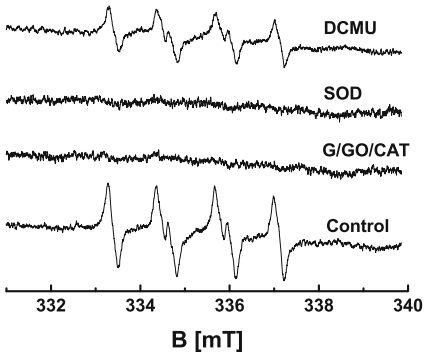

Fig. 3 Effect of G/GOX/CAT, SOD and DCMU on light-induced EMPO-OOH adduct EPR spectra measured in PSII membranes. The EMPO-OOH adduct EPR spectra were recorded by continuous illumination for 90 s with white light (1,000 μmol photons m^{-2} s^{-1}). Removal of molecular oxygen was carried out using 50 U ml^{-1} glucose oxidase, 5 mM glucose and 500 U ml^{-1} catalase. 500 U ml^{-1} SOD and 20 μM DCMU were added to PSII membranes priori to illumination. Other conditions were same as described in the legend of Fig. 2

(2,000 μmol photons m^{-2} s^{-1}) for various time periods (0–180 min). The samples were illuminated on ice with slow stirring. Several aliquots were collected from these samples at various time periods and subjected to detection of $O_2^{\bullet-}$ and $R^{\bullet}$ using EPR spin-trapping spectroscopy.

Heat treatment

PSII membranes (150 μg Chl ml^{-1}) were subjected to heat treatment at 47 °C in a continuous stirring water bath for various time periods in the dark. After completion of heat treatment the samples were immediately transferred on the ice and used for detection of $O_2^{\bullet-}$ and $R^{\bullet}$ using EPR spin-trapping spectroscopy.

EPR spin-trapping EPR

The detection of $O_2^{\bullet-}$ and $R^{\bullet}$ was by accomplished by spin-trapping using EMPO, 5-(ethoxycarbonyl)-5-methyl-1-pyrroline

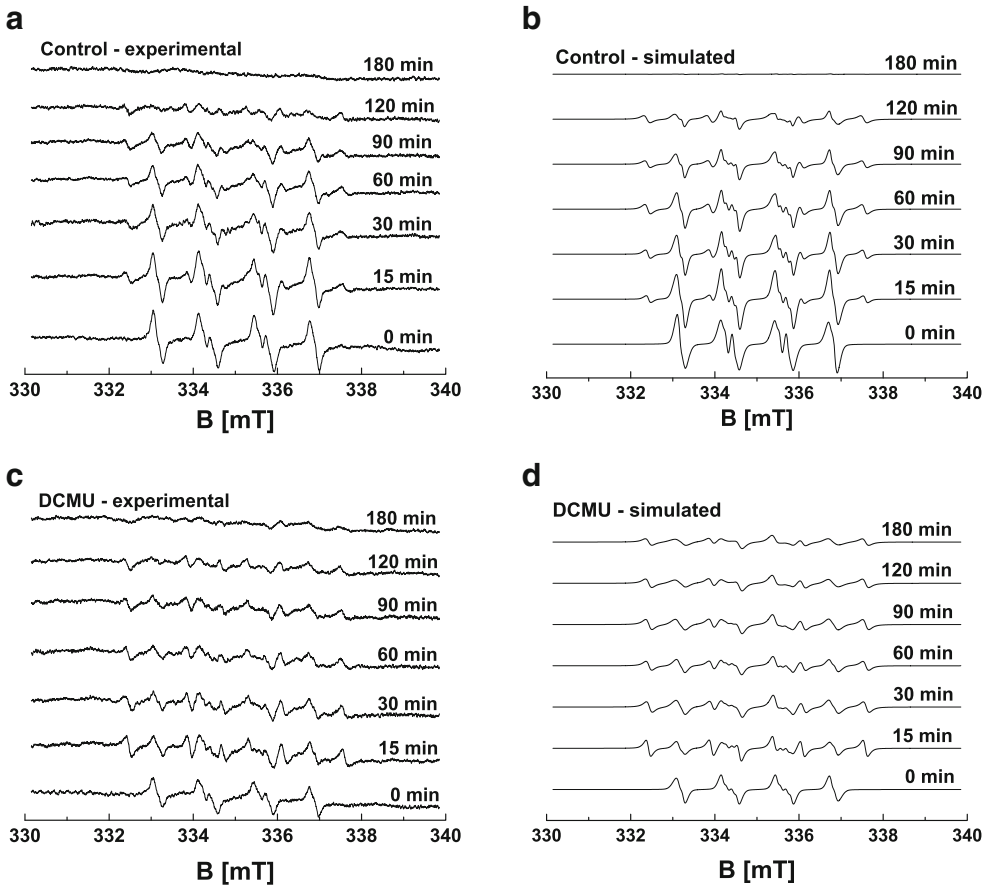

Fig. 4 Experimental (**a**, **c**) and simulated (**b**, **d**) EMPO-OOH and EMPO-R adduct EPR spectra after high light treatment. In (**a**, **c**), light-induced EMPO-OOH and EMPO-R adduct EPR spectra were measured in PSII membranes (150 μg Chl ml^{-1}) previously exposed to high light treatment. High light treatment was carried out by exposure of PSII membranes (150 μg Chl ml^{-1}) to continuous white light (2,000 μmol photons m^{-2} s^{-1}) for various time periods as indicated in the figure. The EMPO-OOH and EMPO-R adduct EPR spectra were recorded after illumination of PSII membranes for 90 s with white light (1,000 μmol photons m^{-2} s^{-1}) in the absence (**a**) and presence (**c**) of 20 μM DCMU. Other conditions were same as described in the legend of Fig. 1. In (**b**, **d**), simulation of experimental EMPO-OOH and EMPO-R adduct EPR spectra observed in PSII membranes previously exposed to high light treatment. Simulation represents linear combinations of the EMPO-OOH adduct (a^N=13.28 G; a^H=11.89 G and a^N=13.28 G; a^H=9.67 G) and EMPO-R adduct (a^N=15.42 G; a^H=22.30 G)

N-oxide (Alexis Biochemicals, Lausen, Switzerland). Figure 1 shows simulated EMPO-OOH and EMPO-R adduct EPR spectra. PSII membranes (150 μg Chl ml^{-1}) in glass capillary tube (Blaubrand® intraMARK, Brand, Germany) were illuminated with continuous white light (1,000 μmol photons m^{-2} s^{-1}) in the presence of 25 mM EMPO, 40 μM desferal and 25 mM Mes (pH 6.5). The strong iron chelator desferal was used to decrease the amount of free iron available for the production of HO$^{\bullet}$ through the Fenton reaction. Illumination was performed using a halogen lamp with a light guide (KL 1500 electronic, Schott, Mainz, Germany) and spectra were recorded using EPR spectrometer MiniScope MS200 (Magnettech GmbH, Berlin, Germany). Signal intensity was evaluated as a relative height of the central doublet of the first derivate of the absorption spectrum. EPR conditions were as follows: microwave power, 10 mW; modulation amplitude, 1 G; modulation frequency, 100 kHz; sweep width, 100 G; scan rate, 1.62 G s^{-1}. Simulation of EPR spectra was done using Winsim software freely available from the website of National Institute of Environmental Health Sciences (2002).

Results

Photogeneration of $O_2^{\bullet-}$ in PSII membranes

The light-induced production of $O_2^{\bullet-}$ in PSII membranes was measured using EPR spin-trapping spectroscopy. The spin-trapping was accomplished by the spin-trapping compound 5-(ethoxycarbonyl)-5-methyl-1-pyrroline N-oxide (EMPO). In non-illuminated sample, the presence of EMPO did not induce any EMPO-OOH adduct EPR signal, whereas illumination with a continuous white light (1,000 μmol photons m^{-2} s^{-1}) resulted in the formation of the EMPO-OOH adduct EPR signal (Fig. 2a). The four line spectrum exhibits all the characteristics of reported EMPO-OOH adduct spectrum (Olive et al. 2000; Zhang et al. 2000). Figure 2a (upper most trace) shows the characteristic EMPO-OOH adduct EPR signal generated by superoxide-generating system xanthine-xanthine oxidase. Time dependence of EMPO-OOH adduct EPR signal shows that $O_2^{\bullet-}$ is gradually produced within the whole period of illumination (Fig. 2b). These results indicate that illumination of PSII membranes results in $O_2^{\bullet-}$ production.

Effect of molecular oxygen, SOD and DCMU on $O_2^{\bullet-}$ photogeneration

To test the origin of $O_2^{\bullet-}$ production, the effect of molecular oxygen, SOD and electron transport inhibitor DCMU on light-induced formation of $O_2^{\bullet-}$ was studied (Fig. 3). When molecular oxygen was removed using glucose/glucose oxidase/catalase system, the formation of $O_2^{\bullet-}$ was completely diminished. Similarly, upon addition of exogenous SOD to PSII membranes prior to illumination EPR signal of the EMPO-OOH adduct was completely diminished. The addition of DCMU, an inhibitor that blocks electron transfer from Q_A to Q_B, resulted in

Table 1 Percentage contribution of EMPO-OOH and EMPO-R adduct EPR signal components identified by decomposition of the simulated composite EMPO adduct EPR spectra. The simulation analysis of experimental EMPO adduct EPR spectra was accomplished using the two spectral components with the following hyperfine coupling constants: a^N=13.28 G; a^H=11.89 G and a^N=13.28 G; a^H=9.67 G (EMPO-OOH adduct) and a^N=15.42 G; a^H=22.30 G (EMPO-R adduct)

High light				Heat			
Time [min]	EMPO-OOH [%]		EMPO-R [%]	Time [min]	EMPO-OOH [%]		EMPO-R [%]
	a^N 13,2 a^H 9,67	a^N 13,2 a^H 11,89	a^N 15,4 a^H 22,3		a^N 13,2 a^H 9,67	a^N 13,2 a^H 11,89	a^N 15,4 a^H 22,3
Control				Control			
0	39,65	60,35	0	0	40,16	59,84	0
15	35,54	56,32	8,14	3	32,56	48,4	19,04
30	28,92	55,22	15,86	4	33,91	43,97	22,12
60	27,11	47,36	25,54	5	32,41	42,61	24,99
90	16,32	41,51	42,17	7	23,52	32,61	43,86
120	12,00	38,24	49,66	10	20,42	28,49	51,09
180	27,87	37,6	34,52				
DCMU				DCMU			
0	36,58	63,42	0	0	44,09	55,91	0
15	17,75	33,54	48,71	3	22,42	32,81	44,78
30	19,75	35,95	44,31	4	21,95	37,16	40,89
60	18,69	34,35	46,96	5	8,89	37,49	53,63
90	17,55	32,12	50,33	7	14,77	27,49	57,74
120	16,64	31,19	52,17	10	10,4	9,41	80,19
180	17,82	35,11	47,07				

approximately half decline in EMPO-OOH adduct EPR signal. These results indicate that $O_2^{\bullet-}$ is formed by one-electron reduction of molecular oxygen on the PSII electron acceptor side.

Photogeneration of $O_2^{\bullet-}$ and $R^{\bullet}$ under photoinhibition

In order to study the effect of high light treatment on the light-induced formation of $O_2^{\bullet-}$, EMPO-OOH adduct EPR spectra were measured in PSII membranes previously exposed to high light treatment. PSII membranes were exposed to strong white light (2,000 μmol photons m^{-2} s^{-1}) for various time periods as indicated in Fig. 4a and c. Subsequently to high light treatment, EMPO spin trap compound was added to PSII membranes and EMPO-OOH adduct EPR signal was induced by continuous illumination for 90 s with white light (1,000 μmol photons m^{-2} s^{-1}) in the absence and presence of DCMU (Fig. 4a and c, respectively).

When the effect of high light treatment on the light-induced formation of $O_2^{\bullet-}$ was measured in the absence of DCMU, the exposure of PSII membranes to high light treatment caused decrease in EMPO-OOH adduct EPR signal (Fig. 4a). Interestingly, the decrease in EMPO-OOH adduct EPR signal was accompanied by the appearance of EMPO-R adduct EPR signal formed by the interaction of EMPO spin trap compound and $R^{\bullet}$. To confirm the spectral distribution of $O_2^{\bullet-}$ and $R^{\bullet}$ in EMPO adduct EPR spectra, the simulation of EMPO adduct EPR spectra was performed (Fig. 4b). The best simulation of experimental data was accomplished using two spectral components with hyperfine coupling constants 1) a^N=13.28 G; a^H=11.89 G and a^N=13.28 G; a^H=9.67 G and 2) a^N=15.42 G; a^H=22.30 G, which are in good agreement with hyperfine coupling constant attributed to EMPO-OOH and EMPO-R adducts, respectively (Stolze et al. 2002). Table 1 shows the percentage contribution of the spectral components identified by decomposition of the simulated composite EMPO adduct EPR spectra. Time profile of EMPO-OOH adduct EPR signal shows that EMPO-OOH adduct EPR signal decreases gradually during the whole period of high light treatment (Fig. 5a, solid circles), whereas EMPO-R adduct EPR signal was formed in the initial period of high light treatment (Fig. 5a, open circles). In agreement with these observations, the decomposition of the simulated composite EMPO adduct EPR spectra shows that the percentage contribution of EMPO-OOH adduct component decreased, whereas EMPO-R adduct component increased. These results reveal that high light treatment of PSII membranes caused gradual suppression of $O_2^{\bullet-}$ production and simultaneous formation of $R^{\bullet}$.

When the effect of high light treatment on the light-induced formation of $O_2^{\bullet-}$ was measured in the presence of DCMU, EMPO-OOH adduct EPR signal was observed to gradually decrease similarly to the absence of DCMU (Fig. 4c). Interestingly, the presence of DCMU in PSII membranes previously exposed to high light treatment caused more pronounced enhancement in the formation of EMPO-R adduct EPR signal as compared to the absence of DCMU. In agreement with experimental data, the simulation of EMPO adduct EPR spectra shows that the percentage contribution of EMPO-OOH adduct component decreased, whereas the percentage contribution of EMPO-R adduct component increased (Fig. 4d, Table 1). Time profile of EMPO-OOH adduct EPR signal shows that EMPO-OOH adduct EPR signal decreased gradually (Fig. 5b, solid squares), whereas EMPO-R adduct EPR signal was formed in the initial period of high light treatment and subsequently gradually decrease in the similar manner as EMPO-OOH adduct EPR signal (Fig. 5b, open squares). Based on these observations, it is suggested that the binding of DCMU to the Q_B-

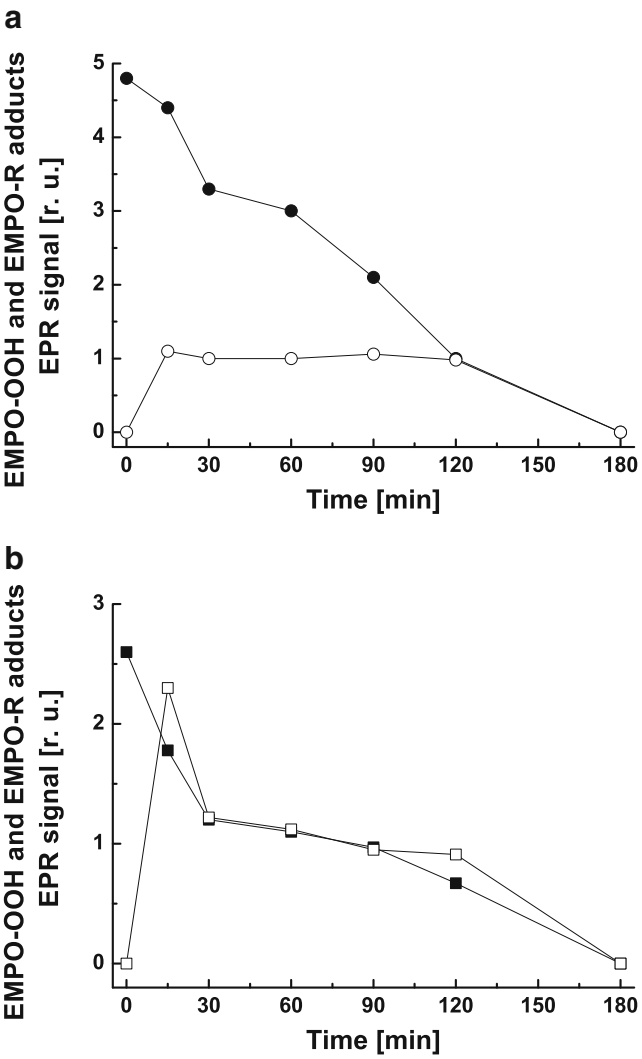

Fig. 5 Dependence of the light-induced EMPO-OOH and EMPO-R adduct EPR signals on the period of high light treatment. The EMPO-OOH (*solid circles*) and EMPO-R (*open circles*) adduct EPR signals were recorded after illumination of PSII membranes for 90 s with white light (1,000 μmol photons m^{-2} s^{-1}) in the absence (**a**) and presence (**b**) of 20 μM DCMU. Signal intensity was evaluated as the relative height of the central doublet of the first derivative of the absorption spectrum

binding site pronouncedly promotes formation of $R^{\bullet}$ after high light treatment.

Photogeneration of $O_2^{\bullet-}$ and $R^{\bullet}$ under heat stress

To explore the effect of heat treatment on the light-induced formation of $O_2^{\bullet-}$, EMPO-OOH adduct EPR spectra were measured in PSII membranes previously exposed to heat treatment. PSII membranes were exposed to heat treatment (47 °C) for various time periods as indicated in Fig. 6a and c. Subsequently to heat treatment, EMPO spin trap compound was added to PSII membranes and EMPO-OOH adduct EPR signal was induced by continuous illumination for 90 s with white light (1,000 μmol photons m^{-2} s^{-1}) in the absence and presence of DCMU (Fig. 6a and c, respectively).

When the effect of heat treatment on the light-induced formation of $O_2^{\bullet-}$ was measured in the absence of DCMU, the exposure of PSII membranes to heat treatment resulted in the decline of EMPO-OOH adduct EPR signal and simultaneous appearance of weak EMPO-R EPR signal (Fig. 6a). In agreement with these observations, the decomposition of the simulated composite EMPO adduct EPR spectra show that the percentage contribution of EMPO-OOH adduct component decreased, whereas EMPO-R adduct component increased (Fig. 6b, Table 1). Time profile of EMPO-OOH adduct EPR signal shows that EMPO-OOH adduct EPR signal decreased gradually (Fig. 7a, solid circles), while a weak EMPO-R EPR signal appeared in the initial period of heat treatment (Fig. 7a, open circles).

When the effect of heat treatment on the light-induced formation of $O_2^{\bullet-}$ was measured in the presence of DCMU, a gradual decrease in EMPO-OOH adduct EPR signal and appearance of weak EMPO-R adduct EPR signal were observed (Fig. 6c). Similarly to high light treatment, the presence

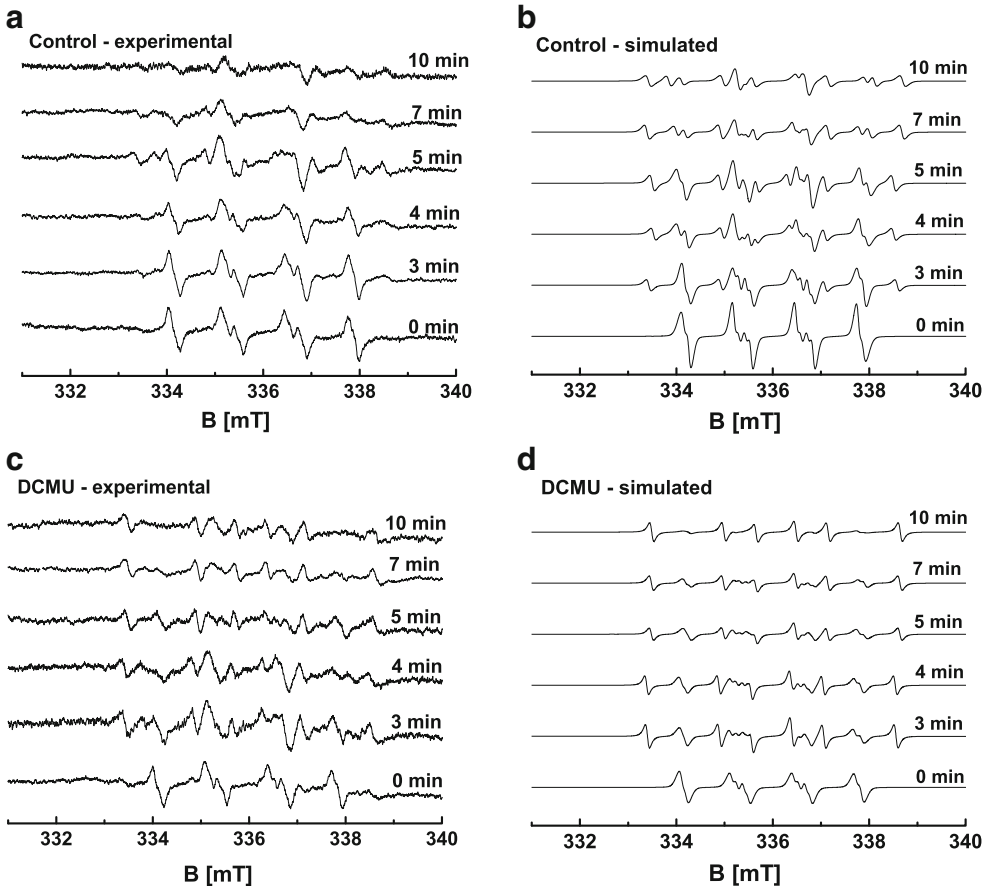

Fig. 6 Experimental (**a**, **c**) and simulated (**b**, **d**) EMPO-OOH and EMPO-R adduct EPR spectra after heat treatment. In (**a**, **c**), light-induced EMPO-OOH and EMPO-R adduct EPR spectra were measured in PSII membranes previously exposed to heat treatment. Heat treatment was carried out by exposure of PSII membranes (150 μg Chl ml^{-1}) to 47 °C for various time periods as indicated in the figure. The EMPO-OOH and EMPO-R adduct EPR spectra were recorded after illumination of PSII membranes for 90 s with white light (1,000 μmol photons m^{-2} s^{-1}) in the absence (**a**) and presence (**b**) of 20 μM DCMU. Other conditions were same as described in the legend of Fig. 1. In (**b**, **d**), simulation of experimental EMPO-OOH and EMPO-R adduct EPR spectra observed in PSII membranes previously exposed to heat treatment. Simulation represents linear combinations of the EMPO-OOH adduct (a^N=13.28 G; a^H=11.89 G and a^N=13.28 G; a^H=9.67 G) and EMPO-R adduct (a^N=15.42 G; a^H=22.30 G)

of DCMU in PSII membranes previously exposed to heat treatment caused more pronounced enhancement in the formation of EMPO-R adduct EPR signal (Fig. 6c) as compared to the absence of DCMU (Fig. 6a). In agreement with experimental data, the simulation of EMPO adduct EPR spectra shows that the percentage contribution of EMPO-OOH adduct component decreased, whereas the percentage contribution of EMPO-R adduct component increased (Fig. 6d, Table 1). Time profile of EMPO-OOH adduct EPR signal shows that EMPO-OOH adduct EPR signal decreased gradually (Fig. 7b, solid squares), whereas EMPO-R adduct EPR signal was formed in the initial period of heat treatment and subsequently remained constant (Fig. 7b, open squares). These observations reveal that the binding of DCMU to the Q_B-binding site markedly stimulates formation of $R^{\bullet}$ after heat treatment.

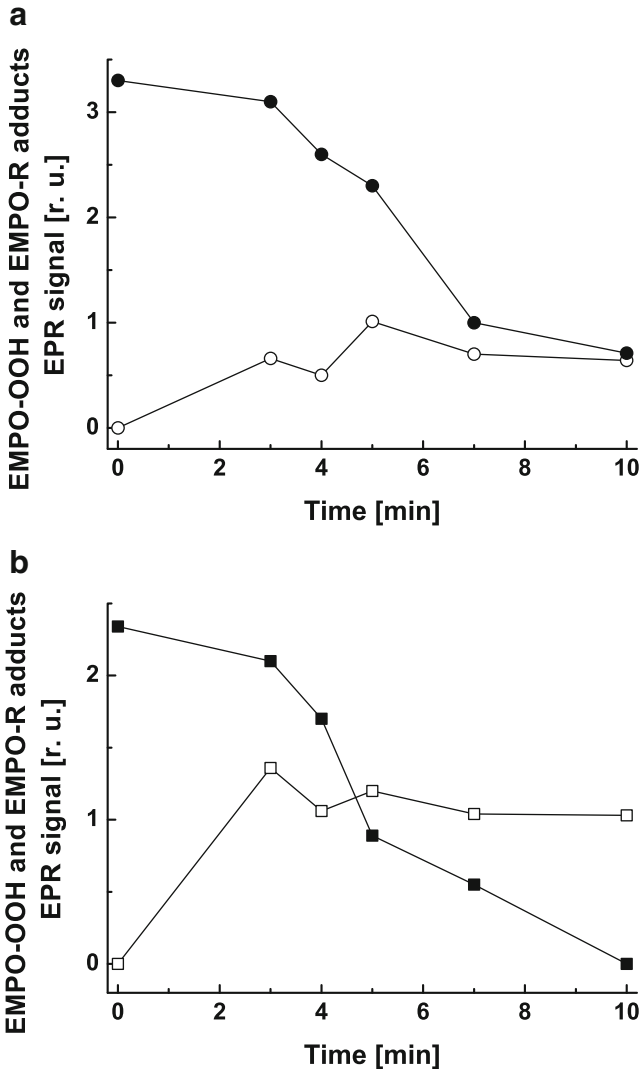

Fig. 7 Dependence of the light-induced EMPO-OOH and EMPO-R adduct EPR signals on the period of heat treatment. The EMPO-OOH (*solid squares*) and EMPO-R (*open squares*) adduct EPR signals were recorded after illumination of PSII membranes for 90 s with white light (1,000 μmol photons m^{-2} s^{-1}) in the absence (**a**) and presence (**b**) of 20 μM DCMU. Signal intensity was evaluated as the relative height of the central doublet of the first derivative of the absorption spectrum

Effect of molecular oxygen and SOD on $R^{\bullet}$ formation under photoinhibition and heat stress

To further characterize light-induced formation of $R^{\bullet}$ after high light and heat treatment, the effect of anaerobic condition and exogenous SOD on the EMPO-R adduct EPR signal was studied. Removal of molecular oxygen using glucose/glucose oxidase/catalase system in the PSII membranes, previously exposed to high light treatment resulted in the complete suppression of $R^{\bullet}$ formation (Fig. 8). Similarly, when molecular oxygen was removed from PSII membranes previously exposed to heat treatment, light-induced formation of $R^{\bullet}$ was diminished (Fig. 8). These observations indicate that molecular oxygen is required for light-induced formation of $R^{\bullet}$ in PSII exposed to both high light and heat treatment.

When SOD was added to the PSII membranes previously exposed to high light treatment, formation of $R^{\bullet}$ was completely diminished (Fig. 8). Similarly, light-induced formation of $R^{\bullet}$ was completely suppressed by exogenous SOD (Fig. 8). These observations indicate that scavenging of $O_2^{\bullet-}$ by exogenous SOD prevents light-induced formation of $R^{\bullet}$ in the PSII membranes exposed to both high light and heat treatment. Based on these results, it is concluded that $O_2^{\bullet-}$ is involved in the formation of $R^{\bullet}$ exposed to both high light and heat treatment.

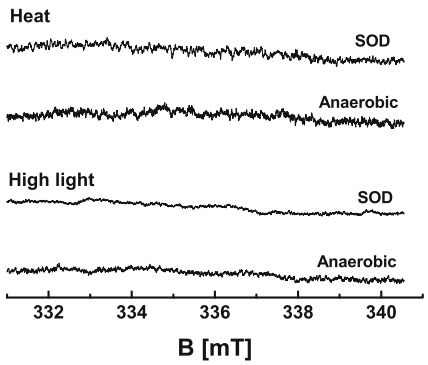

Fig. 8 Effect of SOD and molecular oxygen on light-induced EMPO-OOH and EMPO-R adduct EPR spectra measured in PSII membranes previously exposed to high light and heat treatments. The EMPO-OOH and EMPO-R adduct EPR signals were recorded after illumination of PSII membranes for 90 s with white light (1,000 μmol photons m^{-2} s^{-1}). High light treatment was carried out by exposure of PSII membranes (150 μg Chl ml^{-1}) to continuous white light (2,000 μmol photons m^{-2} s^{-1}) for 30 min. Heat treatment was carried out by exposure of PSII membranes (150 μg Chl ml^{-1}) to 47 °C for 5 min. Removal of molecular oxygen was accomplished using 50 U ml^{-1} glucose oxidase, 5 mM glucose and 500 U ml^{-1} catalase. 500 U ml^{-1} SOD was added to PSII membranes prior to illumination

Discussion

Photoproduction of $O_2^{\bullet-}$ on PSII electron acceptor side

In this study, the light-induced production of $O_2^{\bullet-}$ was studied in PSII membranes. Using EPR spin-trapping spectroscopy, it was demonstrated that illumination of PSII membranes results in the production of $O_2^{\bullet-}$ (Fig. 2). It has been previously demonstrated that $O_2^{\bullet-}$ is produced by one-electron reduction of molecular oxygen on PSII electron acceptor side (Ananyev et al. 1994; Cleland and Grace 1999; Pospíšil et al. 2004, 2006). Apart from PSII electron acceptor side, one-electron oxidation of H_2O_2 on PSII donor side might also contribute to the production of $O_2^{\bullet-}$ (Pospíšil 2009, 2012). Oxidized tyrosines, a $TyrZ^{\bullet}$ (Tyr-161 of subunit D1 of PSII) and $TyrD^{\bullet}$ (Tyr-161 of subunit D2 of PSII) are likely candidates for H_2O_2 oxidation. Our observation that removal of molecular oxygen by glucose/glucose oxidase/catalase system resulted in the complete suppression of EMPO-OOH adduct signal (Fig. 3) indicates that $O_2^{\bullet-}$ is formed by reduction of molecular oxygen on the electron acceptor side of PSII. The observation that DCMU partially prevented $O_2^{\bullet-}$ production (Fig. 3) reveals that the site of $O_2^{\bullet-}$ formation is both prior to and after Q_B-binding site. Even if it is still unclear which of the reduced electron acceptor acts as a donor to molecular oxygen, it is assumed that prior to Q_B-binding site the most likely candidates are highly reducing $Pheo^{\bullet-}$ and tightly bound plastosemiquinone $Q_A^{\bullet-}$, while after Q_B-binding site molecular oxygen is reduced by loosely bound plastosemiquinone $Q_B^{\bullet-}$ and free plastosemiquinone $PQ^{\bullet-}$ (Pospíšil 2009, 2012).

Photoproduction of $R^{\bullet}$ on PSII electron acceptor side

Illumination of PSII membranes previously exposed to high light or heat treatments resulted in the formation of $R^{\bullet}$ (Figs. 4 and 6). The likely candidate for light-induced oxidation of polyunsaturated fatty acids and amino acids are $O_2^{\bullet-}$ and $HO^{\bullet}$. Due to the higher oxidation power of $HO^{\bullet}$ (Em $HO^{\bullet}/H_2O$=2.31 V, pH 7), $HO^{\bullet}$ is more reactive compared to $O_2^{\bullet-}$ (Em $O_2^{\bullet-}/H_2O_2$=0.89 V, pH 7). The observation that the formation of $R^{\bullet}$ was completely suppressed by exogenous SOD confirmed that $O_2^{\bullet-}$ is involved in the production of $R^{\bullet}$ (Fig. 8). Based on the fact that EMPO-R adduct was measured in the presence of strong iron chelator desferal, the involvement of $HO^{\bullet}$ in the light-induced oxidation of polyunsaturated fatty acid or amino acid can be excluded.

It was previously demonstrated that $O_2^{\bullet-}$ is unable to oxidize polyunsaturated fatty acids and amino acids (Aikens and Dix 1991). However, when protons are available in diffusion-limited area, protonation of $O_2^{\bullet-}$ results in the formation of perhydroxyl radical ($HO_2^{\bullet}$) (pKa 4.8). Formation of $HO_2^{\bullet}$ occurs particularly at the surface of the membrane, where the concentration of protons is high. The perhydroxyl radical is oxidizing agent able to directly abstract hydrogen from polyunsaturated fatty acids and amino acids. The higher ability of $HO_2^{\bullet}$ to abstract hydrogen from polyunsaturated fatty acids and amino acids is due to the more oxidizing power (Em of $O_2^{\bullet-}/H_2O_2$ and $HO_2^{\bullet}/H_2O_2$ redox couple is 0.89 V and 1.06 V, respectively) and the lack of negative charge on the molecule. These considerations are in agreement with previous finding that protonated form $HO_2^{\bullet}$ abstracts proton from allylic methylene of polyunsaturated fatty acid, whereas its unprotonated form $O_2^{\bullet-}$ has no such capability (Gebicki et al. 1981).

Based on these considerations, it is concluded that the oxidation of polyunsaturated fatty acids and amino acids by $HO_2^{\bullet}$ on the electron acceptor side of PSII results in the formation of $R^{\bullet}$, which is known to initiate a cascade of reactions leading to the lipid peroxidation and protein degradation.

Acknowledgments This work was supported by the grants no. ED0007/01/01 Centre of the Region Haná for Biotechnological and Agricultural Research and no. CZ.1.07/2.3.00/20.0057 Operational Programme Education for Competitiveness from the Ministry of Education Youth and Sports, Czech Republic. We thank Dr. Jan Hrbáč for support with respect to the EPR measurements.

References

Aikens J, Dix TA (1991) Perhydroxyl radical ($HOO^{\cdot}$) initiated lipid peroxidation. The role of fatty acid hydroperoxides. J Biol Chem 266:15091–15098

Ananyev GM, Renger G, Wacker U, Klimov VV (1994) The production of superoxide radicals and the superoxide dismutase activity of photosystem II. The possible involvement of cytochrome b_{559}. Photosynth Res 41:327–338

Apel K, Hirt H (2004) Reactive oxygen species: metabolism, oxidative stress, and signal transduction. Ann Rev Plant Biol 55:373–399

Asada K (2006) Production and scavenging of reactive oxygen species in chloroplasts and their functions. Plant Physiol 141:391–396

Berthold DA, Babcock GT, Yocum CF (1980) A highly resolved, oxygen evolving photosystem II preparation from spinach thylakoid membranes. FEBS Lett 134:231–234

Bhattacharjee S (2005) Reactive oxygen species and oxidative burst: roles in stress, senescence and signal transduction in plants. Curr Sci 89:1113–1121

Cleland RE, Grace SC (1999) Voltammetric detection of superoxide production by photosystem II. FEBS Lett 457:348–352

Dean RT, Fu S, Stocker R, Davies MJ (1997) Biochemistry and pathology of radical-mediated protein oxidation. Biochem J 324:1–18

Eltsner EF (1987) Metabolism of activated oxygen species. In: Davis DD (ed) The biochemistry of plants. Academic, San Diego, pp 253–315

Ford RC, Evans MCW (1983) Isolation of a photosystem 2 preparation from higher plants with highly enriched oxygen evolution activity. FEBS Lett 160:159–164

Foyer CH (2001) The contribution of oxygen metabolism in photosynthesis to oxidative stress in plants. In: Inze D, Van Montagu M (eds) Oxidative stress in plants. Taylor & Francis, London, pp 33–68

Fridovich I (1998) Oxygen toxicity: a radical explanation. J Exp Biol 201:1203–1209

Gebicki JM, Benon HJ, Bielski BHJ (1981) Comparison of the capacities of the perhydroxyl and the superoxide radicals to initiate chain oxidation of linoleic acid. J Am Chem Soc 103:7020–7022

Halliwell B, Gutteridge JMC (2007) In: Free radicals in biology and medicine. Fourth Edition. Oxford University Press

Hideg É (1999) Free radical production in photosynthesis under stress conditions. In: Pessarakli M (ed) Handbook of plant and crop stress. Marcel Dekker, New York, pp 911–930

Hideg É, Spetea C, Vass I (1994) Singlet oxygen and free radical production during acceptor- and donor-side-induced photoinhibition. Studies with spin trapping EPR spectroscopy. Biochim Biophys Acta 1186:143–152

Hideg É, Spetea C, Vass I (1995) Singlet oxygen production in thylakoid membranes during photoinhibition as detected by EPR spectroscopy. Photosynth Res 46:399–407

Krieger A, Rutherford AW, Vass I, Hideg É (1998) Relationship between activity, D1 loss, and Mn binding in photoinhibition of photosystem II. Biochemistry 37:16262–16269

NIEHS (2002) WinSIM, NIEHS, Research Triangle Park, NC USA. Available at: http://www.niehs.nih.gov/research/resources/software/tools/index.cfm. Accessed on 15 April 2013

Olive G, Mercier A, Moigne FL, Rockenbauer A, Tordo P (2000) 2-ethoxycarbonyl-2-methyl-3,4-dihydro-2H-pyrrole-1-oxide: evaluation of the spin trapping properties. Free Radic Biol Med 28:403–408

Pospíšil P (2009) Production of reactive oxygen species by photosystem II. Biochim Biophys Acta 1787:1151–1160

Pospíšil P (2012) Molecular mechanisms of production and scavenging of reactive oxygen species by photosystem II. Biochim Biophys Acta 1817:218–231

Pospíšil P, Arató A, Krieger-Liszkay A, Rutherford AW (2004) Hydroxyl radical generation by photosystem II. Biochemistry 43:6783–6792

Pospíšil P, Šnyrychová I, Kruk J, Strzałka K, Nauš J (2006) Evidence that cytochrome b_{559} is involved in superoxide production in photosystem II: effect of synthetic short-chain plastoquinones in a cytochrome b_{559} tobacco mutant. Biochem J 397:321–327

Stolze K, Udilova N, Nohl H (2002) Spin adducts of superoxide, alkoxyl, and lipid-derived radicals with EMPO and its derivatives. Biol Chem 383:813–820

Zhang H, Joseph J, Vasquez-Vivar J, Karoui H, Nsanzumuhire C, Martásek P, Tordo P, Kalyanaraman B (2000) Detection of superoxide anion using an isotopically labeled nitrone spin trap: potential biological applications. FEBS Lett 473:58–62